



Protozoa Optimized Deep Perceptual Enhancement Network for Lung CT Imaging

Mahender Erukala¹, Suresh Kumar Sanampudi²

¹Research Scholar, Computer Science and Engineering, JNT University Hyderabad, Telangana, India.

²Professor, Department of Information Technology, JNTUH University College of Engineering Jagtial, Telangana, India.

E-mail: ¹mahee99@gmail.com, ²sureshsanampudi@jntuh.ac.in

Abstract

The precise feature extraction of small details from images of the human body is considered a challenge since fine details like small nodules and delicate vasculature are hard to see while the computed tomography scan is being conducted due to low contrast. Although various contrast enhancement methods have been introduced for better visibility of the images, they generally introduce more noise and edge artifacts. In this paper, a self-supervised Deep Perceptual Enhancement Network with an Artificial Protozoa Optimizer named APO-DPENet is proposed for optimizing the parameters of the image effectively. The results comparing the proposed method with other methods show a PSNR of 25.75308 dB, an SSIM of 0.95894, a CEI of 0.91385, and an EPI of 0.98960 units. The results indicate better contrast retention and edge preservation of the proposed method, along with improved noise removal capabilities. This suggests that the proposed method is robust enough for analysis.

Keywords: Lung CT Enhancement, DPE-Net, Artificial Protozoa Optimizer, Perceptual Quality, Residual Encoder Decoder.

1. Introduction

Although CT scans are frequently used to view the lungs, their inherent contrast or scan resolution limitations may make it more difficult for viewers or algorithms to detect minute nodules or functionally related tissue variations. Although general contrast improvement techniques like HE, CLAHE [1], or the gamma approach might reveal more contrast, these methods might also be accompanied by elevation of the noise level or reduced edges, leading to a balance between detail preservation and homogeneity [2]. Deep convolutional networks (DCNs) are able to learn contextually informed transformations from substandard to high-quality representation data. RED-Net, abbreviation Residual Encoder-Decoder Convolutional Neural Networks, is one of the representative architectures for symmetric encoder-decoder networks with skip link mechanisms, which have been used as a reference architecture in numerous challenges for their ability to refine intricate structures with stable optimization processes [3]. Techniques of residual leaning with skip link mechanisms have also been proven advantageous for noise reduction in CT images for low dose scans [4].

Despite the improvements, there are three major open problems in lung CT image perceptual enhancement: first, existing algorithms are unable to achieve a good balance between maintaining global contrast and preserving edge information and texture details, generating unwanted oversharpening effects [5]. Secondly, the vast majority of existing approaches based on DL techniques rely heavily on paired training data, the amount of such data is actually small in practical clinical usage, while more practical benefit lie in self-supervised approaches that do away with any need for data annotation or predefined masks [6]. Third, the perceptual enhancement visual improvements are highly parameter-dependent, such as network depth, residual learning scale, learning parameters, and trade-offs among loss terms, while their optimization has found relatively little use in existing studies [7, 8]. Despite some improvements, this is a technically challenging area where the noise in the low contrast images in lung CT reduces the minute details that are critical in clinical diagnosis. Despite improvements in existing algorithms, HE, CLAHE, and Gamma Correction only succeed in contrast while blurring edges; the second affects brightness with the possibility of minute texture loss, respectively. Deep learning methods have also shown promising results. However, these methods typically demand a lot of annotated samples in the training set and are sensitive to hyperparameters, causing either smoothing effects or possible artifacts. In our research work, we introduce a self-supervised enhancement technique that combines a light-weight residual network with an APO. The model adjusts the network parameters to find an optimal solution to the contrast enhancement problem while simultaneously keeping the structure intact.

Although many recent studies have been conducted for the purposes of segmentation, classification, and nodule detection in lung CT images, research on image enhancement is still limited. In this context, this proposed work attempts to provide a robust and adaptive image enhancement solution for lung CT images, rigorously tested on the widely used publicly available LIDC dataset, establishing a foundation for future research related to the analysis of the lung image, and the proposed goal of this work concentrates on annotation-free perceptual image enhancement of lung CT images with the purpose of emphasizing the contrast of the images with anatomical veracity [3]. To achieve robustness for various situations, this proposed work utilizes the newest bio-inspired metaheuristic approach named the Artificial Protozoa Optimizer to optimize the parameters of the model via a simulation of the foraging and reproduction processes of protozoa [9]. The assessment procedure involves the use of reference-based fidelity metrics (PSNR and SSIM) and no-reference perceptual measures (contrast improvement index (CII) and edge preservation index (EPI)) commonly found in image enhancement tasks. Relative comparisons are performed with existing standard baselines like HE, CLAHE, gamma, log, and adaptive gamma transforms, as well as with wavelet and RED CNN. The overall research focus of this endeavor is to design a perceptual enhancement framework for low-contrast lung CT images that is adaptive with respect to its defining hyperparameters. The research proposed here has the following overall objectives: (a) design an efficient encoder-decoder network that maintains details of the pulmonary structures, (b) develop an adaptive optimizer based on the notion of protozoa to make the network perceptually adaptive with respect to its contrasting characteristics, and (c) optimize for patient variability in the existing LIDC-IDRI database.

The novelty of the proposed work lies in the application of a common fully self-supervised perception enhancement driven by the developed APO-DPENet approach. This will handle simultaneously the following three challenges not effectively addressed in the state-of-the-art works: i) the contrast structure imbalance problem introduced by the conventional enhancement process, ii) the lack of paired training data for carrying out the lung CT image restoration process, and iii) the instability of the hyperparameters of the residual encoder-

decoder architecture. In contrast to the conventional residual network architecture and other common heuristic optimizers, the proposed APO-DPENet model incorporates an adaptive survival strategy search process with the perceptual residual learning process. This will enable the dynamic adjustment of contrast-sensitive parameters like the residual scale factor, the SSIM weight factor, and the dynamics of the learning process. The remaining sections of this paper will be organized as follows: Section 2 presents some previous research on lung CT enhancement and optimization techniques. Then, section 3 describes the proposed model and methods in detail. The subsequent section explains the experiments, datasets, and results. The final section presents the conclusion and suggests possible future work.

2. Related Work

2.1 Traditional Techniques in Lung CT Images

Traditional models exhibit limitations such as HE, which enhances global contrast by redistributing image intensities but often results in a loss of local structural details and over-enhancement artifacts, CLAHE mitigates some HE drawbacks by working on smaller image regions [10]. However, its performance is strongly dependent on manual parameter tuning (clip limit, tile size), which if improperly set, can induce noise amplification and inconsistent enhancements across images. Gamma, adaptive gamma and log modifications adjust image luminance following a power law but struggle to simultaneously improve contrast and preserve fine anatomical textures [11]. The primary limitation addressed in this study is the inconsistent enhancement of lung CT scans, where existing contrast-modification techniques often amplify noise, distort anatomical boundaries, or fail to preserve subtle textures. Specifically, HE causes global over-stretching of intensities, CLAHE introduces region-dependent contrast imbalance when clip limits are not correctly chosen, and gamma and adaptive gamma frequently blur micro-vascular patterns, while log enhancement exaggerates noise in low-density regions. These limitations collectively demonstrate the necessity for a principled approach that balances global contrast, local texture, and edge fidelity without relying on manual tuning.

2.2 Bio-Inspired Optimizers in Deep Learning

Including residual encoder-decoder networks offers context-driven enhancement and better noise reduction but requires vast annotated datasets for supervised training, which are scarce in medical CT imaging [12]. Without rigorous hyperparameter optimization, these models risk introducing unwanted smoothing or artifacts that degrade diagnostic quality [13].

A large body of work treats contrast enhancement as a search problem and solves it with bio-inspired optimizers. In the Artificial Bee Colony (ABC) [14] line, the intensity-mapping parameters are chosen by maximizing a composite score that balances edge strength, entropy, and overall contrast, yielding consistent gains over hand-tuned baselines [15]. The Selfish Herd Optimizer (SHO) follows a different swarm metaphor, exploring both pixel-level and transform-parameter encodings. The Artificial Protozoa Optimizer (APO) extends this family with exploration-exploitation phases modeled on protozoan behaviors, designed to navigate complex, non-convex search spaces efficiently, which is attractive for deep model and loss hyperparameter tuning [9].

The Artificial Protozoa Optimizer improves on existing bio-inspired optimization methods by more effectively balancing exploration and exploitation in complex search spaces.

Unlike the Artificial Bee Colony (ABC) algorithm which maximizes fixed composite scores, or the Selfish Herd Optimizer (SHO) that combines pixel-level and transform parameter searches, APO mimics the adaptive survival behaviors of protozoa including foraging, dormancy, and reproduction to dynamically adjust its search strategy. This adaptive approach prevents APO from converging too early and allows it to explore the non-convex and high-dimensional parameter spaces common to image enhancement tasks to reliably find hyperparameter configurations that improve contrast and edge details in medical images while reducing noise and artifacts, which is not possible with previous methods that only consider the contrast between pixels. The proposed APO-DPENet combines deep perceptual enhancement with bio-inspired optimization, which is different from previous methods that only consider pixel-level contrast. The use of Artificial Protozoa Optimization ensures dynamic parameter tuning, achieving a balance between contrast improvement and structural preservation.

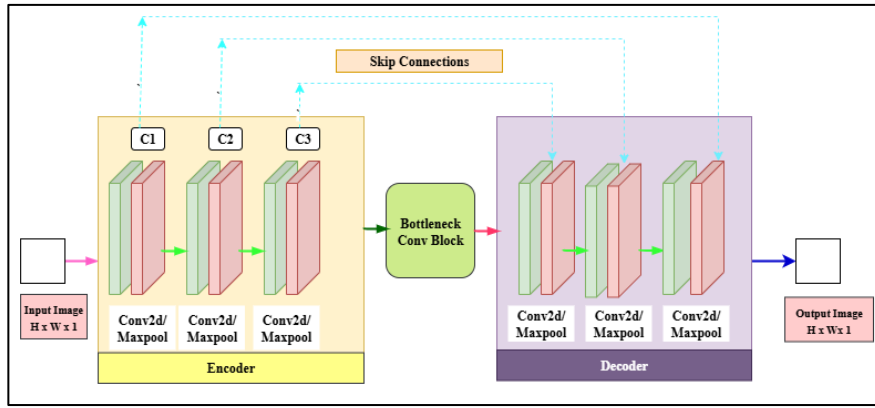


Figure 1. DPENet Architecture for Perceptual Image Enhancement

3. Proposed Work

The definition of lung CT images' perceptual enhancement can be stated as an improvement in the clarity of low contrast slices while maintaining true anatomy and the visibility of small nodules as well as lesions. The proposed light residual encoder-decoder network entails the prediction of a small adjustment mask over the image. Important hyperparameters (base width, residual scale, learning rate, weight decay, λ) are then tuned with APO.

3.1 DPE-Net Architecture

DPE-Net is a compact residual encoder-decoder for single-channel lung CT enhancement. An input slice $X^{[0,1]H \times W}$ passes through a four-stage encoder of convolutional blocks (3×3 kernels with ReLU and reflection padding) interleaved with downsampling, so that features are distilled from fine to coarse scales while the channel width increases. It is started from the lowest resolution and further includes an additional convolution with a 3×3 kernels in the bottleneck section for context acquisition. Additionally, with the upsampling step at every scale and skip connections, symmetry is ensured. This is required for the reversibility of the processing in the decoder stage. Artifacts present in the boundary regions for the checkerboard patterns have been eliminated with the addition of the recovery process capabilities included in the equations. The proposed method of DPENet has been explained in Figure 1.

3.2 Artificial Protozoa Optimizer (APO)

APO is a population-based global optimization approach using four strategies to ensure survival; this can be seen in the living behaviors of protozoa based on autotrophic foraging, heterotrophic foraging, dormancy, or reproduction. The solution to the problem involves protozoa moving through the landscape to solve an objective function with activity varying based on performance. Figure 2 describes the functional process of the APO optimizer.

3.2.1 Autotrophic Foraging (Exploration)

In this case, the individuals make general, stochastic explorations to investigate other parts of the region. The intention is to diversify the population by exploring areas that may be far from the current elites, which elites can be determined by Eq. (1).

$$x_i^{t+1} = x_i^t + \alpha \cdot R_i \quad (1)$$

Where, x_i^t denotes the position of the i^{th} solution at iteration t , x_i^{t+1} is the updated position, α is the exploration step size, R_i is a uniformly sampled random vector.

3.2.2 Heterotrophic Foraging (Exploitation)

When the favorable regions in the search space are identified, the dynamics of the search process tend to develop towards more localized and guided searches. In this process, the solution searches and modifications around regions of high fitness through the use of biased modifications guided by Eq. (2).

$$x_i^{t+1} = x_i^t + \beta \cdot (x_best^t - x_i^t) + \gamma \cdot \varepsilon_i \quad (2)$$

Where, β controls the attraction toward the best solution, γ scales the local random walk, and ε_i introduces Gaussian noise for stochastic refinement.

3.2.3 Dormancy (Stagnation Control)

According to Eq. (3), certain individuals cease searching when the search process is stuck, such as when there is little progress within the prefixed duration of time or when the fitness values are highly stuck. It keeps the data intact, avoids pointless calculations, and then proceeds with changes to the variables' step sizes and/or directions.

$$x_i^{t+1} = x_i^t \quad (3)$$

This mechanism saves computational resources and retains potentially valuable solutions in case stagnation occurs.

3.2.4 Reproduction (Diversity Injection)

The parameters are periodically recombined or mutated to generate new candidates using better performing solutions, in order to introduce diversity into the population of solutions and avoid stagnation in suboptimal solutions, according to Eq. (4).

$$x_{new} = \lambda \cdot x_p + (1 - \lambda) \cdot x_q \quad (4)$$

Here, x_p , x_q are selected parent candidates based on fitness, and λ is a blending coefficient.

3.3 Propose APO-DPENet Model

This paper presents a framework that integrates a bio-inspired optimization method with a lightweight residual encoder-decoder to ensure improved perceived quality of single-channel lung CT images. In DPE-Net, a residual correction $r\theta$ is learned that is modulated by a variable α and is further added to a native slice to improve contrast and preserve anatomical structure. Furthermore, during training, a self-supervised learning method is employed in which a low-contrast image is derived from a native image, and a network is trained on a perception loss function that maximizes contrast correction without compromising anatomical distortion. However, because the performance on image contrast correction is exceedingly parameter-sensitive with a non-convex optimization environment, parameter optimization is a difficult process. To resolve this dilemma, a process called APO is leveraged to search for optimal hyperparameters for significant parameters like base width BBB, residual scale α , and weight parameter λ .

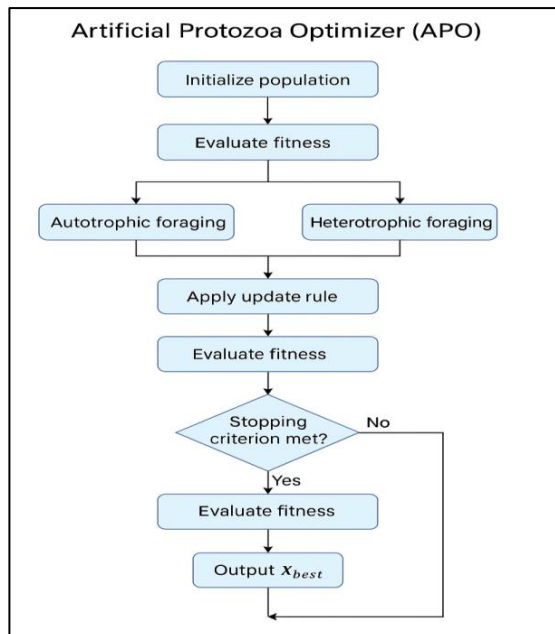


Figure 2. Flowchart of the APO, Showing its Adaptive Search Behavior Inspired by Protozoa Survival Strategies

APO alternates four behaviors based on the model of protozoan survival strategies: autotrophic foraging (world-wide proposals), heterotrophic foraging (refined proposals for interesting regions), dormancy (temporary freeze for stagnated proposals), and reproduction (recombination/mutation of good proposals for diversification). The proposals are trained for a short number of epochs and ranked based on validation loss. The best proposals are refined through an additional training phase with early stopping as a supplement for the DPE-Net optimization strategy. By incorporating APO with DPE-Net, the parameters are adjusted towards maximum perceptual balance for better enhancement of contrasts and margins between nodules and vessels without artifacts in the reproducible method. From experimental results, APO-DPE-Net provides better performance for PSNR/SSIM and CII/EPI compared to conventional algorithms (HE, CLAHE, gamma, log) and DPE-Net without APO, which validates the suitability of the proposed approach for the visual enhancement of lung CT

images. Figure 3 clarifies the methodologies for the proposed model of lung CT image visual enhancement in the following image.

APO utilizes the hyperparameters to update based on the fitness value of each parameter within each iteration. Rather than learning based on fixed values of learning rate and regularization $\{B, \alpha, \lambda, lr, wd\}$ these values are instead adjusted based on progress from the previous iteration. Parameters that give superior results in the perceptual loss are given priority through preference to selection probability, whereas less contributing ones are diminished. The residual predictor checks the continuity of the edge as well as the support of context. Noise edges have isolated gradients without any structure around them. Anatomical edges have directional continuity; thus, anatomical edges are maintained by the residual block while removing noise boundaries.

Algorithm 1: Proposed APO–DPENet

Input: Search bounds for $h=\{B, \alpha, \lambda, lr, wd\}$, APO population N .

Output: Best hyperparameters h^* .

Step 1: grayscale \rightarrow optional percentile clip \rightarrow min–max to $[0,1]$ \rightarrow resize (e.g., 128×128).

Step 2: Self-supervised pair: for each slice x , sample ϕ and form $x' = T\phi(x)$ (bounded gamma/ contrast/ brightness).

Step 3: sample N hyperparameter sets $\{h_i^0\}$ within bounds; for each h_i^0 , train DPE-Net for a few epochs with early stopping and record validation loss.

Step 4: APO loop ($t = 1 \dots T$)

- Behavior select per candidate (autotrophic exploration / heterotrophic exploitation / dormancy / reproduction).
- Propose h_i^t using the chosen operator, clip to bounds.
- Short train DPE-Net under h_i^t (few epochs); compute $J(h_i^t)$.
- Elitist update: keep the better of h_i^{t-1} and h_i^t ; track global best h^* .
- Adapt behavior probabilities using recent improvement/diversity.

Step 5: Select h^* best validation risk from APO.

Step 6: Train DPE-Net under h^* to convergence with early stopping \rightarrow obtain θ^*, α^* .

Step 7: Enhanced image.

Step 8: End.

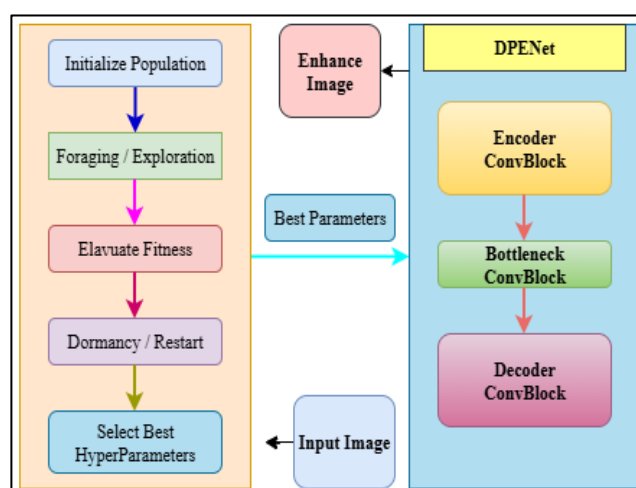


Figure 3. Proposed APO-DPENet Structure for Lung CT Image Perceptual Enhancement

3.3.1 Dataset Description

The proposed research work employs a pre-processed dataset of lung images from a Kaggle repository based on the Lung Image Database Consortium and Image Database Resource Initiative (LIDC-IDRI) [16]. The dataset includes annotations of thoracic computed tomography images for 1,018 patients from expert readers, with a maximum of four masks for each nodule. The dataset is organized based on identifiers for patients and nodules with each nodule analyzed based on volume representations and corresponding masks. The images were sliced from PNG images of the original DICOM images. The pre-processed dataset consists of 15,200 computed tomography images after the rejection of incomplete nodules, corrupted images, and images with a limited number of images. The images were uniformly resized to 128×128 pixels suitable for the input of the proposed model. Variations in the thickness of the images result in variations in the quality of the computed images. The proposed model maintains consistency with a potentially diminished strength of enhancement for thicker sliced images. Figure 4 shows the proposed images.

3.3.2 Implementation Details

CT slices are processed to obtain single-channel maps that are min-max normalized to $[0,1]$ and resized to 128×128 . Conventional techniques like HE with the OpenCV predefined function on 8-bit CT slices converted to grayscale images; CLAHE with a clip limit of 2.0 and a tile-grid size of (8×8) ; Gamma correction with an exponent $\text{gamma}=0.8$ log transformation with a gain parameter of 1.0; and adaptive gamma correction with gamma in the range (0.6-1.6) and a gamma value of 1.1. Others like DPE-Net employ a four-stage residual encoder-decoder architecture with i.e. $\text{Conv3x33} + \text{ReLU}^*2$ with reflection padding and MaxPool2x2 ; two layers of Conv3x3 in a bottleneck; a symmetrical decoder with bilinear upsampling and skip connections by concatenation; a residual head with size 1×1 and a learnable coefficient ' α '; and no batch normalization. Self-supervised learning examples constitute a native slice ' x ' degraded by bounded transformations ' $T\phi$ ', 'contrast', and 'brightness'; with a 'smooth local dimming' option. Optimization algorithms use (learning rate lr , weight decay wd), mini-batches, and early stopping on a validation split, with the best model saved. Critical hyperparameters $h=\{B, \alpha, \lambda, lr, wd\}$ were chosen from the outer loop APO: using exploration, exploitation, dormancy, reproduction operators and elitist selection. In sensitivity analysis, learning rate and λ (perceptual content weight balance) had the greatest sensitivity on PSNR and SSIM. Learning rate values slightly altered the model convergence speed, whereas λ significantly influenced the preservation of texture details. Batch size and α were moderately sensitive, but weight decay was relatively less sensitive.

To achieve the reproducibility of the results, a strictly executed split of the patient-level data was ensured. In this case, the data was split such that 70% of the patients were used to form the training data, with the remaining 15% each being assigned to the validation and test data, preventing contamination of the slices across the groups. Methods of image pre-processing included the use of percentiles, clipping at the 1st and 99th percentiles along with rescaling to a spatial resolution of 128×128 pixels. Regarding to the training methods for DPE-Net, the Adam optimizer was used with a batch size of 8 and a cosine schedule learning rate, training the model for 60 epochs with early stopping based on the SSIM value on the validation data. To facilitate the reproducibility of the experiment, fixed values for the random seeds initializing the models and the data shuffles at the 42nd seed value were ensured. The APO was implemented using a population size of 20 solutions, along with an exploration to exploitation

ratio of 0.6 to 0.4, running the algorithms for up to 35 generations with early stopping determined from the validation loss values. The model parameters were limited to the following ranges the batch size parameters B considered were 16, 32, and 64 units; the search parameter α varied from 0.1 to 1.0; the regularization parameter λ varied from 0.1 to 1.5; the learning rate lr varied from 1×10^{-5} to 1×10^{-3} ; and the weight decay parameter varied from 1×10^{-6} to 1×10^{-4} . The traditional baseline methods had a full parameter search via a grid search for fair comparison of results. In the deep learning paradigm, the RED-CNN model is trained for a total of 50 epochs with the Adam optimizer and a fixed lr of 1×10^{-4} . The Wavelet and TV methods were adjusted for optimal parameter values based on the validation metric of the validation set specific to the SSIM index. To ensure fairness in comparison and analysis of results, parameter tuning for the Wavelet/TV approaches and RED-CNN was conducted using the identical validation set employed for parameter tuning for the proposed approach. The parameter tuning of the baseline approaches did not utilize the APO searching process, but they followed a similar grid search process.

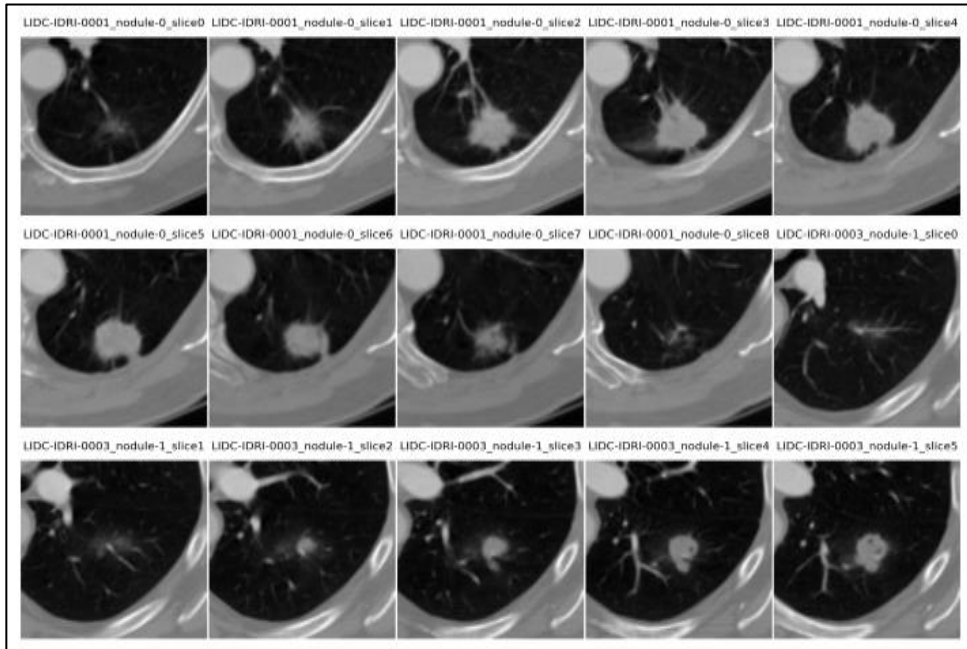


Figure 4. Sample LIDC-IDRI Lung CT Images Used for Contrast Enhancement

3.3.3 Evaluation Metrics

As a measure to quantify the quality of the enhanced images, two fidelity measures and two perceptual quality measures have been employed. The two fidelity measures are PSNR and SSIM; the two perceptual quality measures used here are CII, contrast gain, which is a global measure, and EPI, edge preservation. PSNR and SSIM determine the closeness of the enhanced image to the original image (native slice). CII and EPI determine the contrast gain.

3.3.4 Peak Signal-to-Noise Ratio (PSNR)

Fidelity measure derived from the mean-squared error (higher is better [dB]) as given in the Eq. (5).

$$PSNR(y, x) = 10 \log_{10} (MAX^2 / MSE_{(x,y)}) \quad (5)$$

Where, $x, y \in [0,1]H \times W$, PSNR_mean (dB) higher closer to the reference, and PSNR_std variability of PSNR across images smaller more consistent.

3.3.5 Structural Similarity Index (SSIM)

Perceptual fidelity that jointly measures luminance, contrast, and structure as given in Eq. (6).

$$SSIM(y, x) = \frac{((2\mu_y\mu_x + C1)*(2\sigma_{yx} + C2))}{((\mu_y^2 + \mu_x^2 + C1)*(\sigma_y^2 + \sigma_x^2 + C2))} \quad (6)$$

Let μ_y, μ_x be local means, σ_y^2, σ_x^2 local variances, and σ_{yx} local covariance, higher is better.

3.3.6 Contrast-Improvement Index (CII)

Global contrast gain relative to the original (CII > 1 indicates increased contrast, interpret alongside fidelity metrics to avoid over-enhancement as given in Eq. (7).

$$CII(y, x) = \sigma(y)/\sigma(x) \quad (7)$$

Where CII_mean is 1, it means global contrast has increased. CII_std indicates the variability of contrast gain; smaller values represent better enhancement. CII < 1 indicates a controlled contrast improvement that avoids excessive amplification, whereas values significantly above 1 imply over-enhancement. Therefore, CII values closer to 1 are preferred.

3.3.7 Edge-Preservation Index (EPI)

Correlation between edge magnitude maps of y and x, closer to 1 indicates better edge retention. Define $e_y = G(y)$, $e_x = G(x)$ as follows Eq. (8).

$$EPI(y, x) = \frac{\sum_{u,v} ((e_y - \bar{e}_y) * (e_x - \bar{e}_x))}{\sqrt{\sum_{u,v} ((e_y - \bar{e}_y)^2 * \sum_{u,v} ((e_x - \bar{e}_x)^2)}} \quad (8)$$

where $G(\cdot)$ is a high-pass/edge operator. EPI value near 1 denotes faithful edge preservation; values >1 signal oversharpening and values <1 indicate edge loss.

4. Results and Discussion

It is applied to the same set of images for the independent test subset of the LIDC dataset. Quantitative assessment was done based on the raw results of the network without visualization normalization. Results are provided as mean \pm SD for the tested images. Fidelity assessment utilized PSNR, while perceptual and structural details are quantified in terms of contrast improvement index (CII) and edge preservation index (EPI), respectively but as observed from the perspective of the image. For the evaluation metric configuration, the APODPE-Net achieved better reconstruction quality, namely 25.75 ± 0.59 dB and SSIM of 0.9589 ± 0.036 , displaying better performance than all other approaches considered together. In comparison to the results of the APODPE-Net, the PSNR and SSIM of the traditional

approaches of HE, CLAHE, Gamma, Log, and Adaptive Gamma are generally much lower. Performance variations demonstrate the superiority of the content-aware approach in preserving structural detail more accurately. In global contrast, APO-DPENet achieves the highest contrast (CII 0.91385 ± 0.01912) compared to Wavelet (1.1255 ± 0.075) and RED-CNN (1.0937 ± 0.298). From the edge preservation index, it can be inferred that the approaches follow distinct behavior patterns: for APO-DPE-Net, it is 0.98960 ± 0.00700 , which relates to the over-sharpening approach; for DPE, it is 1.04789 ± 0.01081 , which relates to the mild over-sharpening approach; for Wavelet.

The CII results have been re-evaluated for this purpose; a number slightly below 1 indicates controlled enhancement with global contrast enlargement without reducing the natural appearance of CT images, and the values above 1 indicate over-enhancement and not superiority. The tradeoff between CII values and near-neutral EPI values indicates the appropriateness of the proposed model for clinical assessment. According to the above definitions, the proposed APO-DPENet model demonstrates controlled contrast enhancement with CII = 0.91 and near-zero edge preservation with EPI = 0.98. It satisfies the requirement for clinical propriety and is not inferior. Results indicate consistency with the subjective assessment regarding the visual comparison results: the proposed approach of APO-DPE-Net captures subtle lesions and vessels with a slight hint of mild ringing artifact effects at sharply transitional areas; Wavelet preserves the edge pattern with crisp details and contrast; and RED-CNN eliminates streak artifacts at the cost of reducing the sharpness of edges.

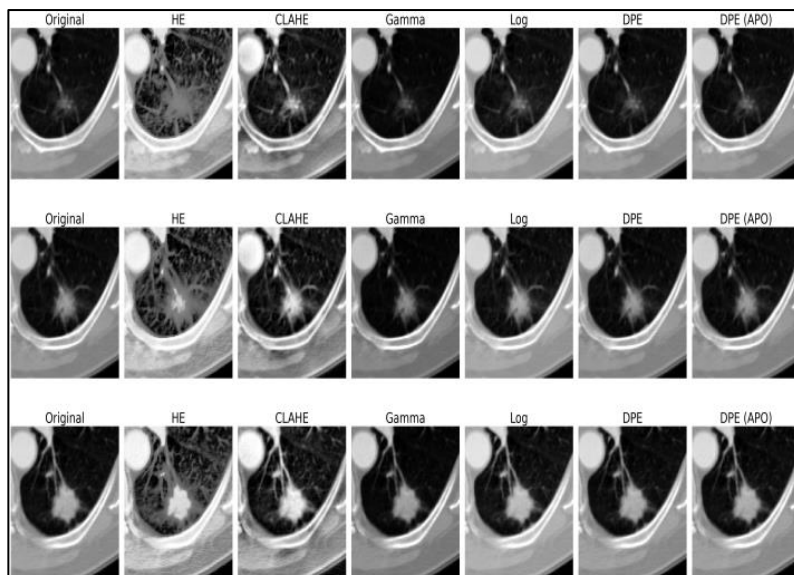


Figure 5. Enhanced Lung CT Images obtained by Different Techniques. The proposed APO-DPE Method Produces Improved Clarity and Detail Preservation

APO-DPENet performs better than Wavelet/TV, RED-CNN, and the conventional methods for the LIDC test set in terms of fidelity of results as well as global contrast. The edge-preserving ability of the network can be optimized for a neutral enhancement boost that also provides a structure-preserving boost, which can be optimal for visual inspection within a clinical setting, while not affecting the increases in PSNR and SSIM values. The quantitative performance of the various enhancement algorithms for PSNR, SSIM, CII, and EPI is provided in T1 and T2. The proposed APO-DPENet shows the best PSNR and SSIM with smaller variability, which indicates its superior performance in enhancement tasks. Figure 6 shows the CT images of lung nodules employing the color-mapping visualization approach for structural illumination.

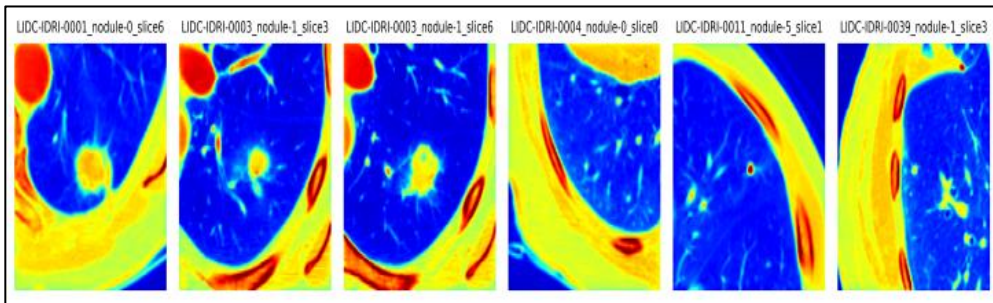


Figure 6. Color-Mapped Representation of further Improved Lung CT Nodules

Table 1 presents the mean values of the quantitative metrics, which directly compare the average enhancement performance between the methods.

Table 1. Comparative Quantitative Evaluation of Image Enhancement Techniques Using PSNR, SSIM, CII, and EPI Metrics

Method	PSNR mean	SSIM mean	CII mean	EPI mean
HE	11.53649	0.44411	1.31896	2.40563
CLAHE	17.72978	0.68468	1.18091	1.90604
GAMMA	19.51005	0.87645	0.92270	0.90040
LOG	19.96248	0.87438	1.10300	1.11439
Adaptive Gamma	20.20883	0.88399	1.04567	1.09429
Wavelet Transform [11]	21.14340	0.84600	1.12550	0.99080
RED CNN [4]	21.81095	0.82200	1.09372	0.79987
DPE	22.29008	0.88598	1.09651	1.04789
Proposed Method	25.75308	0.95894	0.91385	0.98960

The standard deviation of the metrics shown in Table 2 may be useful for testing the stability of the different techniques of image enhancement. The mean and standard deviation values of the PSNR are depicted in Figures 7 and 8, which show that the suggested APO-DPENet model has better quality in the reconstructed output with less variability.

Table 2. Quantitative Std. Performance Comparison of Enhancement Methods across PSNR, SSIM, CII, and EPI Metrics

Method	PSNR std	SSIM std	CII std	EPI std
HE	1.75960	0.10048	0.16730	0.64022
CLAHE	0.62778	0.03870	0.07898	0.13842
GAMMA	0.80726	0.03820	0.02672	0.03855
LOG	0.94926	0.06716	0.02761	0.03717
Adaptive Gamma	0.83556	0.05565	0.03922	0.07378
Wavelet Transform [11]	0.71461	0.07154	0.07511	0.07610
RED CNN [4]	0.69867	0.08241	0.29815	0.02561
DPE	0.63390	0.03663	0.01538	0.01081
Proposed Method	0.59455	0.03612	0.01912	0.00700

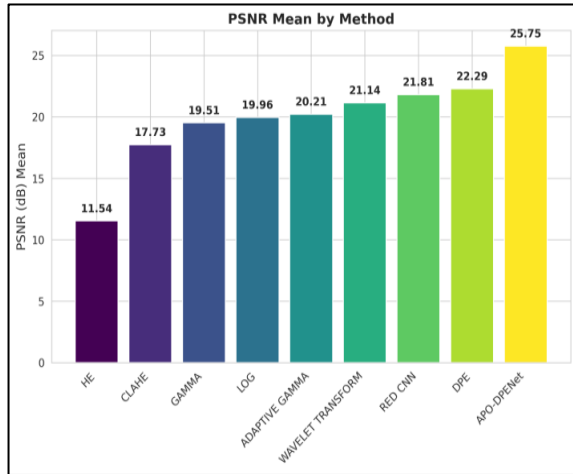


Figure 7. Mean PSNR Performance Evaluation of Different Image Enhancement Techniques

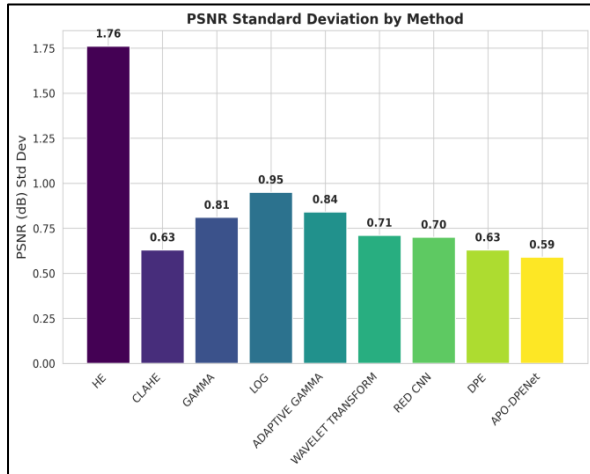


Figure 8. PSNR Standard Deviation Detailed Examination of Image Enhancement Methods

The Figures 9 and 10 exhibit the mean and standard deviation of SSIM, emphasizing that APO-DPENet preserves structural similarity with minimal deviation across images.

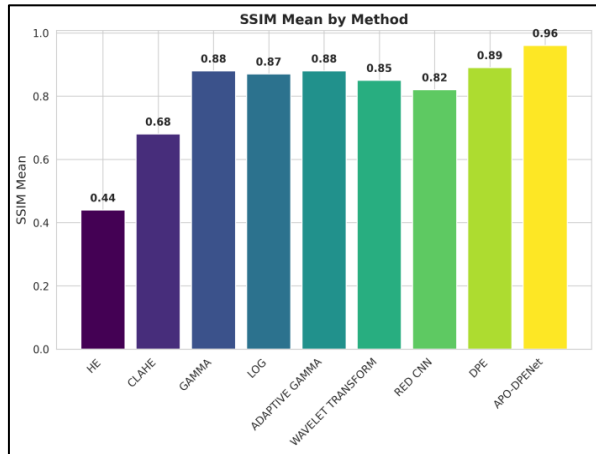


Figure 9. Mean SSIM Performance Evaluation of Different Image Enhancement Techniques

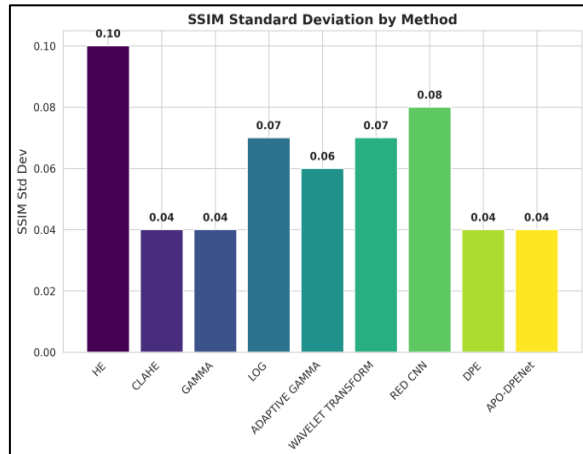


Figure 10. SSIM Standard Deviation Analysis of Image Enhancement Methods

The mean and standard deviation of the Contrast Improvement Index (CII) are illustrated in Figures 11 and 12, where it can be observed that the proposed method is able to improve contrast effectively and efficiently. The mean and standard deviation of the Edge Preservation Index (EPI) are illustrated in Figures 13 and 14, where it can be observed that APO-DPENet is able to preserve edges effectively and has lower variance than other methods in terms of edge preservation. The comparison among different methods for overall performance using heatmap-based normalization for each figure (PSNR, SSIM, CII, and EPI) is illustrated in Figure 15, where it can be observed that APO-DPENet outperforms other conventional and learning-based methods in terms of overall enhancement quality and robustness. Under some conditions for certain lesions in contact with pleural boundary lesions, it may focus more on pleural boundary lesions; hence, mild over-enhancement around pleural boundary lesions may occur. The encoder-decoder structure is succinct; however, it may have some difficulties with irregular lesions like cavitations and multilobulated lesions.

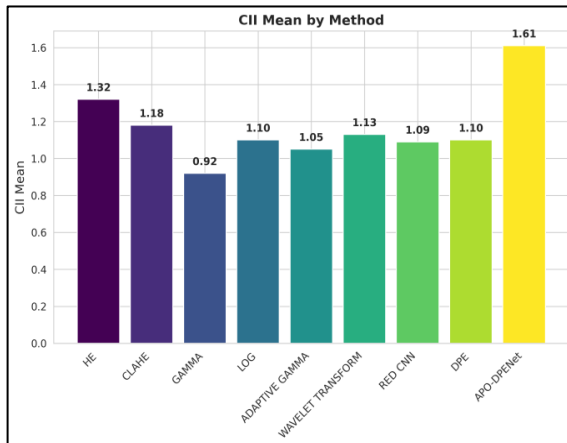


Figure 11. Mean CII Performance Evaluation of Different Image Enhancement Techniques

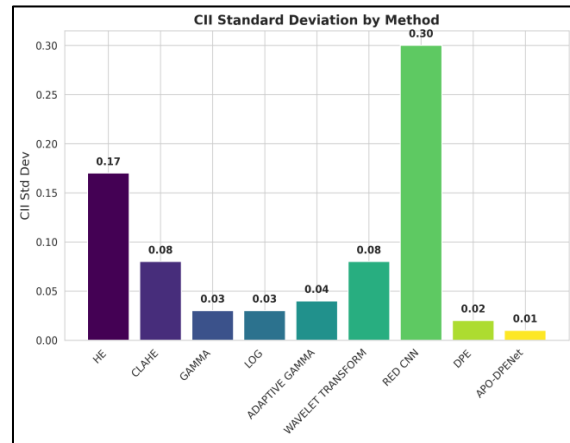


Figure 12. CII Standard Deviation Analysis of Image Enhancement Methods

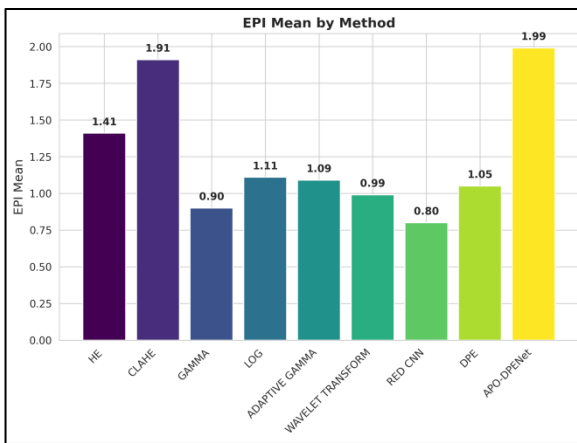


Figure 13. Mean EPI Performance Evaluation of Different Image Enhancement Techniques

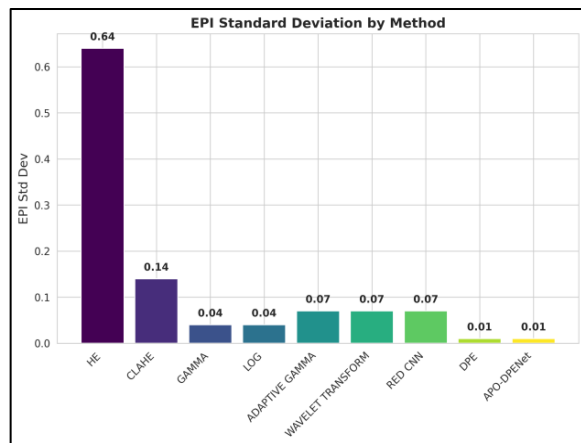


Figure 14. EPI Standard Deviation Analysis of Image Enhancement Methods

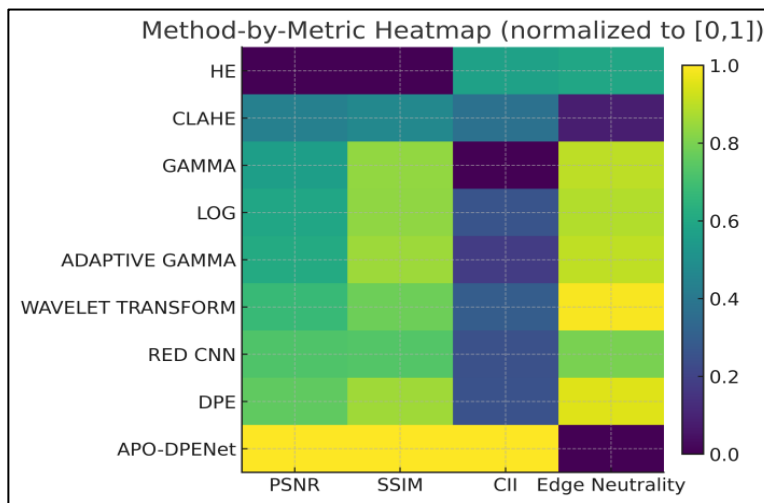


Figure 15. Normalized Metric-Wise Performance Comparison of Image Enhancement Techniques

5. Conclusion

It proposes a self-supervised enhancement approach that seeks a balance between enhancing the quality of lung CT images and preserving some of the anatomical details. With

the adaptive product operation function and residual encoder-decoder structure, the most important parameters can be optimized to achieve the best trade-off between contrast enhancement and image details for this method. The PSNR and SSIM values of the proposed APO-DPENet with optimized parameters outperform the state-of-the-art approaches with an improvement of 3-4 dB and 7-10%, respectively. Second, APO can indeed ensure stable model behavior across slices with no need for any annotations. Moreover, these results prove the scientific interest of the proposed approach, because it is a reproducible, self-supervised, hyperparameter-optimized method for perceptual image enhancement as a pre-processing technique for nodule detection, segmentation, and visualization tasks for precise details in the lung area. This study presents opportunities for future upgrades, where a complete exploitation of 3D CT volumes would make it feasible to achieve a high level of consistency throughout space between slices, as well as potentially overcoming texture artifacts.

References

- [1] Mohammed, Ibrahim Majid, and Nor Ashidi Mat Isa. "Contrast Limited Adaptive Local Histogram Equalization Method for Poor Contrast Image Enhancement." *IEEE Access* (2025).
- [2] Kuran, Umut, and Emre Can Kuran. "Parameter Selection for CLAHE Using Multi-Objective Cuckoo Search Algorithm for Image Contrast Enhancement." *Intelligent Systems with Applications* 12 (2021): 200051.
- [3] Panetta, Karen, Shreyas Kamath KM, Shishir Paramathma Rao, and Sos S. Agaian. "Deep Perceptual Image Enhancement Network for Exposure Restoration." *IEEE Transactions on Cybernetics* 53, no. 7 (2022): 4718-4731.
- [4] Chen, Hu, Yi Zhang, Mannudeep K. Kalra, Feng Lin, Yang Chen, Peixi Liao, Jiliu Zhou, and Ge Wang. "Low-Dose CT with a Residual Encoder-Decoder Convolutional Neural Network." *IEEE transactions on medical imaging* 36, no. 12 (2017): 2524-2535.
- [5] Guha, Ritam, Imran Alam, Suman Kumar Bera, Neeraj Kumar, and Ram Sarkar. "Enhancement of Image Contrast Using Selfish Herd Optimizer." *multimedia tools and applications* 81, no. 1 (2022): 637-657.
- [6] Han, Dong, Liang Li, Xiaojie Guo, and Jiayi Ma. "Multi-Exposure Image Fusion Via Deep Perceptual Enhancement." *Information Fusion* 79 (2022): 248-262.
- [7] Braik, Malik. "Hybrid Enhanced Whale Optimization Algorithm for Contrast and Detail Enhancement of Color Images." *Cluster Computing* 27, no. 1 (2024): 231-267.
- [8] Zhou, Yuanping, Changqin Shi, Bingyan Lai, and Giorgos Jimenez. "Contrast Enhancement of Medical Images Using a New Version of the World Cup Optimization Algorithm." *Quantitative imaging in medicine and surgery* 9, no. 9 (2019): 1528.
- [9] Wang, Xiaopeng, Václav Snášel, Seyedali Mirjalili, Jeng-Shyang Pan, Lingping Kong, and Hisham A. Shehadeh. "Artificial Protozoa Optimizer (APO): A Novel Bio-Inspired Metaheuristic Algorithm for Engineering Optimization." *Knowledge-based systems* 295 (2024): 111737.

- [10] Erukala, Mahender, and Suresh Kumar Sanampudi. "Lumbar Spine MRI Images Quality Enhancement through Contrast Limited Adaptive Histogram Equalization." In 2024 5th International Conference on Communication, Computing & Industry 6.0 (C2I6), IEEE, 2024, 1-6.
- [11] Wang, Hongfei, Ping Yang, Chuan Xu, Lei Min, Shuai Wang, and Bing Xu. "Lung CT Image Enhancement Based on Total Variational Frame and Wavelet Transform." International Journal of Imaging Systems and Technology 32, no. 5 (2022): 1604-1614.
- [12] Zhang, Xiaowen, Yongfeng Ren, Guoyong Zhen, Yanhu Shan, and Chengqun Chu. "A Color Image Contrast Enhancement Method Based on Improved PSO." Plos one 18, no. 2 (2023): e0274054.
- [13] Sharif, S. M. A., Rizwan Ali Naqvi, Mithun Biswas, and Woong-Kee Loh. "Deep Perceptual Enhancement for Medical Image Analysis." IEEE Journal of Biomedical and Health Informatics 26, no. 10 (2022): 4826-4836.
- [14] Chen, Jia, Weiyu Yu, Jing Tian, Li Chen, and Zhili Zhou. "Image Contrast Enhancement Using an Artificial Bee Colony Algorithm." Swarm and Evolutionary Computation 38 (2018): 287-294.
- [15] Abdulkadhim, Ahmed Abd Ali, and Amir Lakizadeh. "Hybrid Parallelism Image Encryption Algorithm Based on a Modified Blowfish Algorithm." International Journal of Intelligent Engineering & Systems 17, no. 6 (2024).
- [16] Armato III, Samuel G., Geoffrey McLennan, Luc Bidaut, Michael F. McNitt-Gray, Charles R. Meyer, Anthony P. Reeves, Binsheng Zhao et al. "The Lung Image Database Consortium (LIDC) and Image Database Resource Initiative (IDRI): A Completed Reference Database of Lung Nodules on CT Scans." Medical physics 38, no. 2 (2011): 915-931.